DOI 10.1007/s10946-023-10175-1
Journal of Russian Laser Research, Volume 44, Number 6, November, 2023

KERR EFFECT AS A MODE LOCKER IN Er-DOPED FIBER LASER

Yu Chen,[1,2] Ahmad Haziq A. Rosol,[3] Sin Jin Tan,[4] Zian Cheak Tiu,[5] Kaharudin Dimyati,[1] and Sulaiman Wadi Harun[1*]

[1] *Department of Electrical Engineering, University of Malaya Kuala Lumpur 50603, Malaysia*

[2] *Chongqing Vocational Institute of Engineering North and South Avenue 1, Binjiang New City, Jiangjin District, Chongqing 402260, China*

[3] *Malaysia–Japan International Institute of Technology (MJIIT), Universiti Teknologi Malaysia Jalan Sultan Yahya Petra, Kuala Lumpur 54100, Malaysia*

[4] *School of Engineering, UOW Malaysia KDU University College Shah Alam 40150, Selangor, Malaysia*

[5] *Faculty of Engineering and Quantity Surveying, INTI International University Negeri Sembilan, Malaysia*

Corresponding author e-mail: swharun @ um.edu.my

Abstract

We propose and demonstrate a passively mode-locked all-fiber laser utilizing a multimode interference effect in graded-index multimode fiber (GIMF). The mode-locking is obtained due to the Kerr effect in GIMF, which induces the intensity modulation inside the ring cavity laser. We obtain stable soliton mode-locked pulses at a center wavelength of 1574.1 nm, with a fixed repetition rate of 22 MHz and a pulse duration of 650 fs, when the pump power is changed in the range from 66.2 to 140.0 mW. The maximum average output power and pulse energy are recorded at 9.82 mW and 448 pJ, respectively, at a pump power of 140 mW. This proves that a nonlinear optical response in GIMF can be used as a new modulation mechanism for obtaining ultra-short pulses based on all-fiber ring cavity.

Keywords: mode locking, Kerr effect, graded-index multimode fiber, soliton.

1. Introduction

Mode-locked fiber lasers (MLFLs) have received a significant attention in recent years owing to their merits in terms of compactness, reliability, high stability, and cost-effectiveness as they are compared to other types of ultrafast lasers [1]. They are also capable to produce short, highly-intense pulses in the picosecond-to-femtosecond range, which are needed in various field of applications, including material science, telecommunications, and bio-photonics [2–6]. Conventionally, MLFLs are realized, using active techniques, which require bulky and complex electronic devices. Passive techniques are simpler, compact, and can be realized at low cost; thus, they have gained interest in recent years [7]. Thin-film saturable absorber (SA) has been normally used in passive techniques. It is an optical component that exhibits a specific level of the light absorption, that reduces at high optical intensities [8]. Several SAs have

Manuscript submitted by the authors in English on September 28, 2023.

been proposed in the literature, including carbon nanotubes (CNTs), graphene, and transition metal dichalcogenides (TMDs) [9, 10]. CNTs possess distinct advantages when compared to traditional SAs [11], including their ease of fabrication, compatibility with fibers, and low cost. They have a remarkably fast recovery time of smaller than a picosecond [12]. But, the use of CNTs is limited by the complexity associated with controlling their band gaps, which restricts their operation to specific wavelengths [13].

The introduction of graphene has diminished the dominance of CNTs due to its ultrafast response time and wide-bandwidth operation [13]. However, graphene has the weaknesses of low modulation depth per layer, complex fabrication processes, and high cost [1, 14]. Other two-dimensional (2D) materials, such as topological insulators [15], black Phosphorus [16], transition metal dichalcogenides [17], and MXene [18] have been demonstrated as SA, since they are not only exhibited wide-band operation and an ultrafast SA property, but also have unique thickness-dependent band gap. But the relatively low optical-damage threshold and gradually degraded characteristics of these SAs are the major problems in practical applications.

Alternatively, the nonlinear effect in the optical fiber-based laser cavity could also be deployed to produce MLFLs. In this paper, we demonstrate a soliton MLFL, using a new mode-locking method based on multimode interference in graded-index multimode fiber (GIMF). The laser is constructed by incorporating GIMF in all-fiber ring cavity to exploit the self-imaging effect in the multimode waveguide. The cavity exhibits nonlinear saturable absorption property to generate femtosecond pulses via mode locking. This approach has advantages of its inherently-high optical-damage threshold, wavelength independence, and all-fiber setup.

2. Preparation of SMS Structure and Laser Setup

At first, a section of graded-index multimode fiber (GIMF) was directly spliced with standard single-mode fiber (SMF) on each side to develop the SMF-GIMF-SMF structure. The GIMF is 45 mm in length with a core diameter of 50 μm and a cladding diameter of 125 μm. In Fig. 1, we show a schematic diagram of the SMF-GIMF-SMF structure.

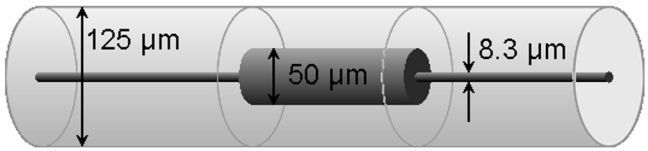

Fig. 1. The SMS structure with a GIMF length of 45 mm.

In Fig. 2 a, we demonstrate the spectral transmission characteristic of the GIMF obtained by launching an amplified spontaneous emission (ASE) source into the structure. Here, a periodic interference pattern obtained due to multimode interference (MMI) induced by several excited modes in the process of the laser light propagation in the GIMF. We also investigate a nonlinear response function of the GIMF with peak power growth due to launching an amplified ultrashort pulse into the SMF-GIMF-SMF structure; see Fig. 2 b. One can see a modulation depth of 4.6% and a saturable intensity of 19.33 MW/cm^2.

A schematic diagram of the laser cavity is illustrated in Fig. 3. The continuous-wave laser diode (LD) provides a maximum output power of 350 mW at 975 nm (II-VI, Model LC96Z400-74). The LD is spliced with a 980/1550 nm wavelength division multiplexer (WDM). A 2 m long Erbium-doped fiber (EDF, Fibercore I25) acting as the gain medium is connected to the cavity after the WDM. The EDF

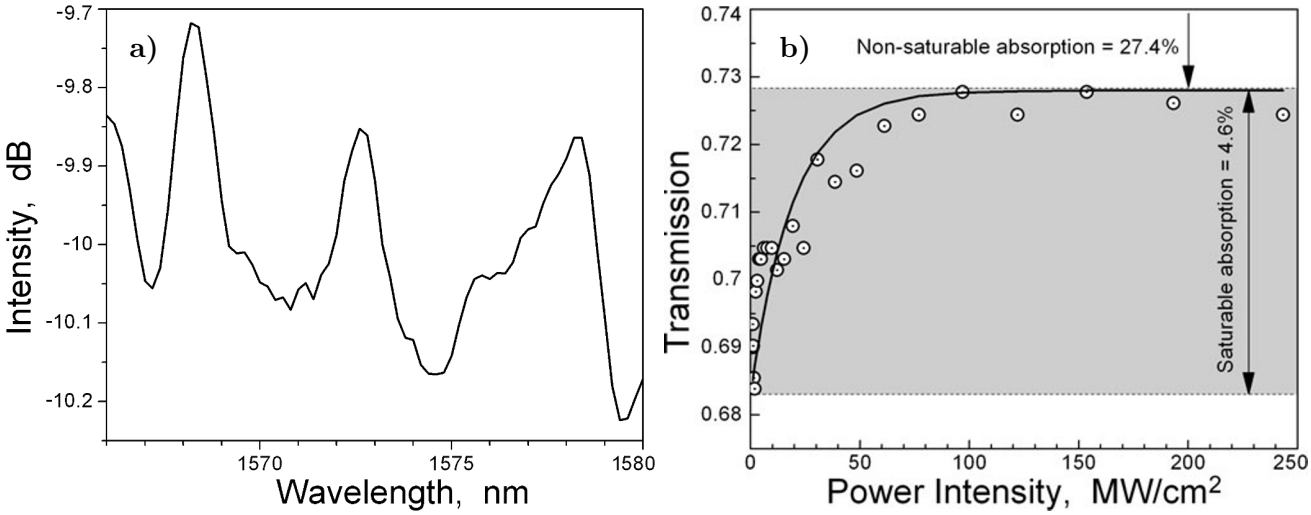

Fig. 2. The spectral transmission characteristic of the SMS structure with a GIMF length of 45 mm in the range of 1566 to 1580 nm (a) and the nonlinear response function with a peak power growth (b).

has a group velocity dispersion (GVD) of 27.6 ps^2/km and an absorption rate 23 dB/m at 980 nm. The output of gain medium is then linked to an isolator to warrant a unidirectional operation of the laser light. The prepared SMF-GIMF-SMF structure is fusion spliced into the cavity to act as SA. It consists of two types of fibers with different core diameters: 8.3/125 μm SMF and 50/125 μm GIMF, which establish mismatched cross-sections at the splicing point. This mismatching not only produces a splicing loss but also causes the mode excitation at the input end and mode coupling at the output end of GIMF. As the light unidirectionally oscillates in the ring cavity, the mode excitation and coupling lead to the wavelength-dependent transmission; see Fig. 2 a. The MMI filtering effect is strongly dependent on the effective refractive index in the fiber's core; thus, it can act as an artificial saturable absorber to modulate the cavity loss for mode locking.

An 80 : 20 coupler is placed after the SMF-GIMF-SMFas feedback to the cavity and output port. The total length of the cavity is about 6.8 m, which includes the gain medium, GIMF, and the single-mode fibers used in the optical components. The cavity net dispersion is calculated to be -0.05 ps^2. The polarization controller positioned before the GIMF can slightly adjust the effective length of the multimode waveguide and, thus, synchronously adjust the transmission or filtering characteristic of the SMF-GIMF-SMF structure. The mode proportion of the pulse, which determines the operating regime of the laser, is also adjusted by the change of the effective length of GIMF [13]. 20% of the oscillating laser is tapped out via the optical coupler (OC) for temporal and spectral analysis, using an optical spectrum analyzer (OSA, Yokogawa, AQ6317C), an oscilloscope (GWINSTEK GDS-3352, 350 MHz bandwidth) with a photodetector (Thorlabs: DET01CFC), a radio-frequency (RF) spectrum analyzer (Anritsu MS2683A, 7.8 GHz bandwidth), and an autocorrelator (Alnair Lab, HAC-200).

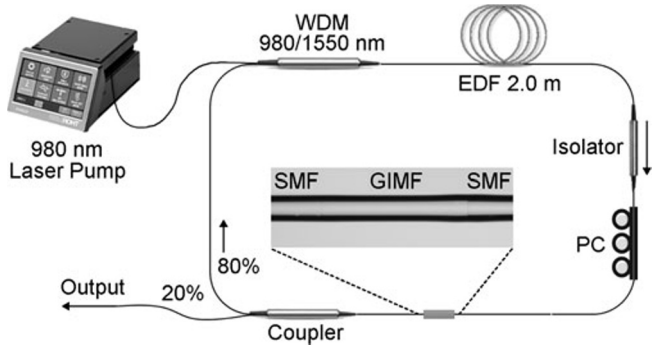

Fig. 3. Schematic cavity design of the MLFL.

3. Result and Discussion

The laser cavity generates a continuous wave (CW) laser light, when it is pumped with an LD power (LDP) of 12 mW. As LDP reached 66.2 mW, it generates mode-locked pulses, and the mode-locking (ML) operation is maintained as the pump power is further increased up to 140.0 mW. The ML operation is due to the MMI, which happens due to the interference of the excited modes in a 45 mm long GIMF, when the single-mode light from the SMF is coupled into the multimode fiber. The superposition of the excited modes produces self-imaging effect in the GIMF. This effect provides a reliable modulation to achieve nonlinear saturable absorption properties of light. The Kerr effect induces the nonlinear change of the refractive index in the laser cavity which, in turn, it results in a change of the self-imaging position or wavelength in the GIMF. Consequently, it slightly changes the transmitted light spectrum of the SMF-GIMF-SMF structure. Since the transmission increases at high laser power, it produces a loss modulation effect like a SA in the laser cavity. ML laser operation is realized at a wavelength, where the SMF-GIMF-SMF structure performs like a saturable absorber. However, the pulses on the OSC ceased to exist as the LDP is increased above 140.0 mW up to a maximum LDP of 350 mW due to the saturation effect. The

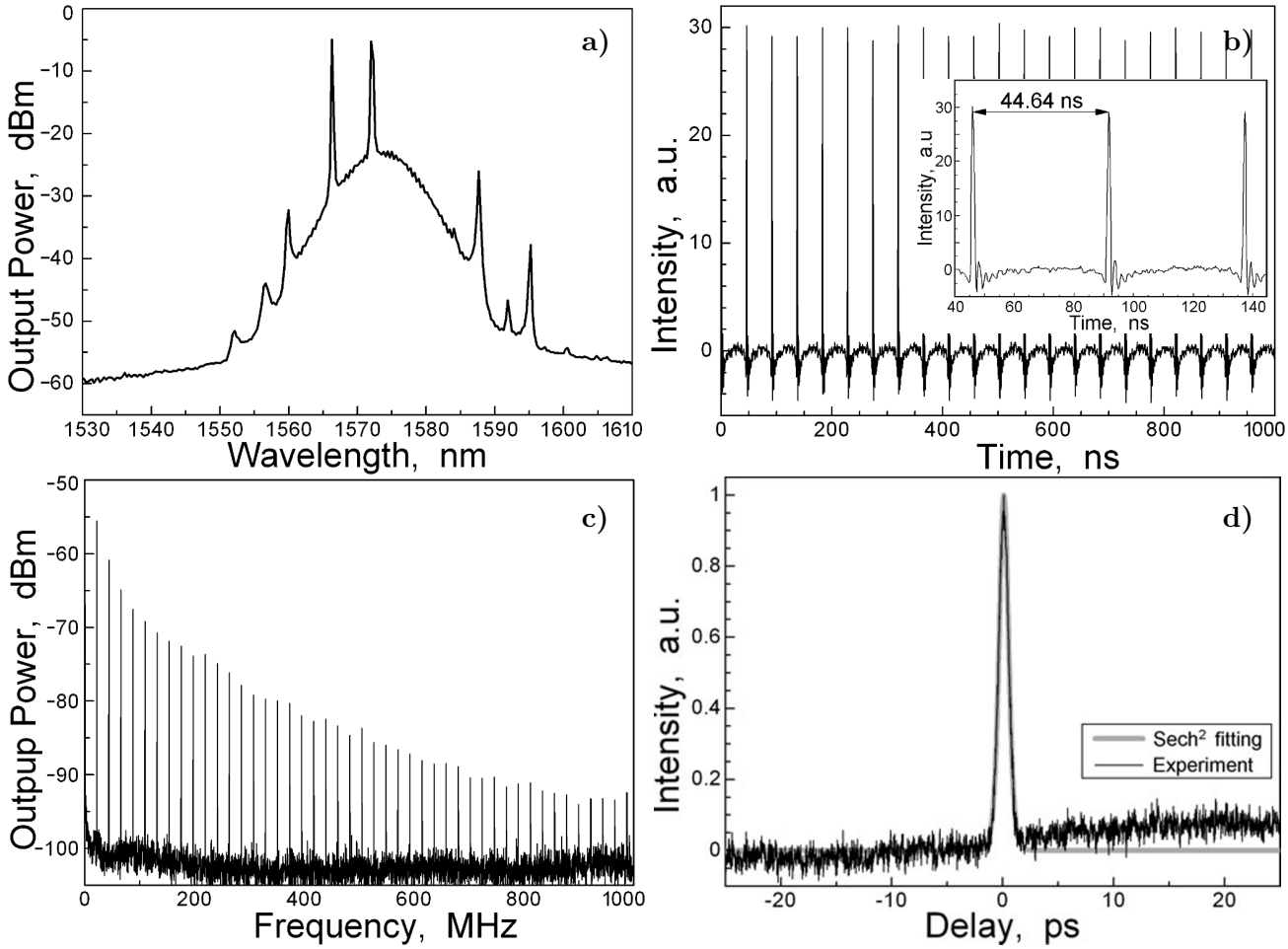

Fig. 4. OSA trace (a), OSC trace (b), RF trace (c), and autocorrelator trace (d).

laser operation reverted to the CW mode, with no pulsing observed in the OSC. By decreasing the LDP to and below 140.0 mW, we observe the reappearance of pulse operation, indicating that the damage threshold of the system exceeded this level, 350 mW.

In Fig. 4 a, we show the output spectrum; the spectrum is centered at 1574.1 nm with a 3 dB spectral bandwidth of 9.0 nm. Few Kelly sidebands are visible in the spectrum, indicating the laser generated soliton pulses. In Fig. 4 b, we present the OSC trace. The pulses exhibit a uniform distribution, indicating a highly stable laser operation. A measured pulse period of 44.64 ns, which corresponds to the 22 MHz repetition rate and matches with the length of the cavity. The RF spectrum within a 1000 MHz span is given in Fig. 4 c. It depicts the fundamental frequency at 22 MHz with a signal-to-noise ratio (SNR) of 43 dB. The high SNR and large number of harmonics that cover a wide radio frequency spectrum up to 1000 MHz indicate the stability of ML operation. We did not find other extra frequency components within the wide spectrum region. In Fig. 4 d, we show that the measured autocorrelation width of an ML pulse is 1.00 ps, which deconvolves to a 650-fs pulse duration assuming a sech^2 pulse shape. Based on the pulse duration and 3 dB spectral bandwidth, the time bandwidth product is calculated to be 0.708. This indicates that the ML pulses are slightly chirped. When the LDP is varied from 66.2 to 140.0 mW, the average output power and pulse energy linearly increase from 3.97 to 9.82 mW and 181 to 448 pJ, respectively; see Fig. 5. The laser has a slope efficiency of 8.0%.

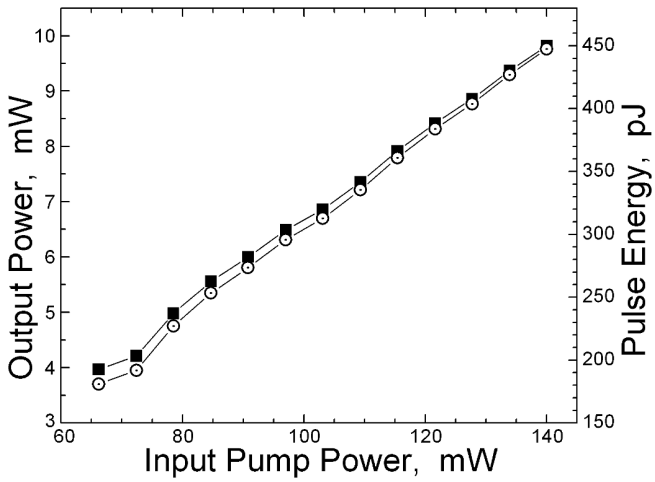

Fig. 5. Pulse energy (⊙) and output power (■) versus LDP.

4. Conclusions

We successfully demonstrated a new ML mechanism, using the Kerr effect of MMI in GIMF. A stable soliton MLFL operating at 1574.1 nm was achieved with a repetition rate of 22 MHz and a pulse duration of 650 fs, using a self-imaging effect in GIMF. We recorded an average output power of 9.82 mW and a pulse energy of 448 pJ at a pump power of 140 mW. This new ML mechanism could be deployed to produce ultrashort pulses in all-fiber laser configuration at any wavelength regions.

Acknowledgments

This study was supported by the Ministry of Higher Education of Malaysia under Prototype Research Grant No. PRGS/1/2022/TK04/UM/01/1.

References

1. N. A. M. Muhammad, N. A. Awang, and H. Basri, *Optik*, **283**, 170855 (2023); DOI: 10.1016/j.ijleo.2023.170855
2. A. Bartels, R. Gebs, M. S. Kirchner, and S. A. Diddams, *Opt. Lett.*, **32**, 2553 (2007).
3. N. Ji, J. C. Magee, and E. Betzig, *Nat. Methods*, **5**, 197 (2008).

4. S. Liu, X. Wu, D. Jung, et al., *Optica*, **6**, 128 (2019).
5. C. Kerse, H. Kalaycıoğlu, P. Elahi, et al., *Nature*, **537**, 84 (2016).
6. P. Elahi, O. Akcaalan, C. Ertek, et al., *Opt. Lett.*, **43**, 535 (2018).
7. Y. Han, Y. Guo, B. Gao, et al., *Prog. Quantum Electron.*, **71**, 100264 (2020).
8. A. Isomaki, "Ultrafast Fiber Lasers Using Novel Semiconductor Saturable Absorbers and Photonic-Crystal Dispersion Compensators," PhD Thesis, Tampere University of Technology (2007).
9. J. Liu, J. Xu, and P. Wang, *Opt. Commun.*, **285**, 5319 (2012).
10. D. Popa, Z. Sun, T. Hasan, et al., *Appl. Phys. Lett.*, **98**, 073106 (2011).
11. D. Lin, K. Xia, R. Li, et al., *Opt. Lett.*, **35**, 3574 (2010).
12. Y.-C. Chen, N. R. Raravikar, L. S. Schadler, et al., *Appl. Phys. Lett.*, **81**, 975 (2002); DOI: 10.1063/1.1498007
13. Q. L. Bao, H. Zhang, Y. Wang, et al., *Adv. Funct. Mater.*, **19**, 3077 (2009); DOI: 10.1002/adfm.200901007
14. J. Li, H. Luo, B. Zhai, et al., *Sci. Rep.*, **6**, 30361 (2016).
15. H. Haris, M. Batumalay, S. J. Tan, et al., *Crystals*, **12**, 489 (2022).
16. A. M. Markom, S. J. Tan, A. R. Muhammad, et al., *Optik*, **223**, 165635 (2020).
17. A. A. Latiff, N. A. Kadir, E. I. Ismail, et al., *Opt. Commun.*, **389**, 29 (2017); DOI:10.1016/j.optcom.2016.12.011
18. A. A. A. Jafri, A. H. A. Rosol, N. Kasim, et al., *Appl. Opt.*, **59**, 8759 (2020).